A Compact Scheme for the Streamfunction Formulation of Navier-Stokes Equations

D. Fishelov[1], M. Ben-Artzi[2], and J.-P. Croisille[3]

[1] Tel-Aviv Academic College for Engineering
218 Bnei-Efraim St., Tel-Aviv 69107
and Beit Berl College
daliaf@post.tau.ac.il
[2] Institute of Mathematics
The Hebrew University, Jerusalem 91904, Israel
mbartzi@math.huji.ac.il
[3] Department of Mathematics
University of Metz, Metz, France
croisil@poncelet.univ-metz.fr

Abstract. We introduce a pure-streamfunction formulation for the incompressible Navier-Stokes equations. The idea is to replace the vorticity in the vorticity- streamfunction evolution equation by the Laplacianof the streamfunction. The resulting formulation includes the streamfunction only, thus no inter-function relations need to invoked. A compact numerical scheme, which interpolates streamfunction values as well as its first order derivatives, is presented and analyzed.

1 Introduction

In a previous study [2] we introduced a new methodology for tracking vorticity dynamics, which is modeled by the incompressible Navier-Stokes equations. Let $\Omega \subseteq R^2$ be a bounded domain with smooth boundary $\partial\Omega$. Recall the vorticity-velocity formulation of the Navier-Stokes equations[3].

$$\partial_t \xi + (\mathbf{u} \cdot \nabla)\xi = \nu \Delta \xi \quad \text{in } \Omega, \tag{1.1a}$$

$$\nabla \cdot \mathbf{u} = \mathbf{0} \quad \text{in } \Omega, \mathbf{u} = \mathbf{0} \ \text{ on } \partial\Omega, \tag{1.1b-c}$$

where $\mathbf{u} = (u, v)$ is the velocity vector, $\xi(\mathbf{x}, t) = \nabla \times \mathbf{u} = \partial_x v - \partial_y u$ is the vorticity field and ν is the viscosity coefficient. Since the flow is incompressible, there exists a streamfunction, ψ, such that $\mathbf{u}(\mathbf{x}, t) = \nabla^{\perp}\psi = \left(-\frac{\partial \psi}{\partial y}, \ \frac{\partial \psi}{\partial x}\right)$, hence the following vorticity-streamfunction relation holds.

$$\Delta \psi = \xi, \quad \mathbf{x} \in \Omega, \quad \psi(\mathbf{x}, t) = \frac{\partial}{\partial n}\psi(\mathbf{x}, t) = 0, \ \mathbf{x} \in \partial\Omega. \tag{1.2}$$

Note that the boundary conditions in (1.2) are due to the no-slip boundary condition $\mathbf{u}(\mathbf{x}, t) = \mathbf{0}, \ \mathbf{x} \in \partial\Omega$.

V. Kumar et al. (Eds.): ICCSA 2003, LNCS 2667, pp. 809–817, 2003.

Equations (1.1)-(1.2) contain two boundary conditions for the streamfunction ψ but no boundary condition for the vorticity ξ. The methodology presented in [2] is to evolve the vorticity in time according to (1.1), and then project the vorticity onto $\Delta(H_0^2(\Omega)) =$ the image of $H_0^2(\Omega)$ under Δ. Relation (1.2) is carried out by applying the Laplacian operator on (1.2), resulting in

$$\Delta^2\psi = \Delta\xi,\ \psi \in H_0^2(\Omega). \tag{1.3}$$

Indeed, (1.3) is a well posed problem, and can be easily approximated by standard numerical schemes. Based on [2], Kupferman [5] introduced a central-difference scheme for the pure-streamfunction formulation.In this paper we construct a pure-compact scheme for the streamfunction formulation. The advantage of the streamfunction formulation of the Navier-Stokes equations is that there is no need to invoke inter-functions relations. Our scheme is based on Stephenson's [7] scheme for the biharmonic equation, where the values of the streamfunction ψ and its first-order derivatives ψ_x and ψ_y serve as interpolated values. We then show that the convective term may be approximated by standard finite difference schemes applied on the first-order derivatives of ψ.

2 Pure-Streamfunction Formulation

Here, we propose a pure-streamfunction formulation. This is obtained by substituting $\xi = \Delta\psi$ and $\mathbf{u}(\mathbf{x},t) = \nabla^{\perp}\psi$ in the vorticity-evolution equation (1.1a). We obtain

$$\frac{\partial(\Delta\psi)}{\partial t} + (\nabla^{\perp}\psi)\cdot\nabla(\Delta\psi) = \nu\Delta^2\psi,\ \mathbf{x}\in\Omega \tag{2.1a}$$

with the boundary conditions

$$\psi(\mathbf{x},t) = \frac{\partial}{\partial n}\psi(\mathbf{x},t) = 0,\ \mathbf{x}\in\partial\Omega. \tag{2.1b}$$

Equations (2.1a)-(2.1b) form a well posed problem.

Theorem 2.1:

$$\|\,|\nabla\psi(\mathbf{x},t)|\,\|_{L^2(\Omega)} \le e^{-2\nu\lambda t}\|\,|\nabla\psi(\mathbf{x},0)|\,\|_{L^2(\Omega)},$$

where λ is a positive constant, which depends on Ω.

3 The Numerical Scheme

To simplify the exposition, assume that Ω is a rectangle $[a,b]\times[c,d]$. We lay out a uniform grid $a \le x_0 < x_1 < ... < x_N = b$, $c \le y_0 < y_1 < ... < y_M = d$. Assume that $\Delta x = \Delta y = h$.

Our approximation in time we apply a Crank-Nicolson scheme to approximate (2.1a) in time.

Our approximation in space is based on Stephenson's [7] scheme for the biharmonic equation

$$\Delta^2\psi = f.$$

Altas et. al. [1] and Kupferman [5] applied Stephenson's scheme, using a multigrid solver. Stephenson's compact approximation for the biharmonic operator is the following.

$$\begin{aligned}(\Delta_h^2)^c\psi_{i,j} = \tfrac{1}{h^4}\{&56\psi_{i,j} - 16(\psi_{i+1,j} + \psi_{i,j+1} + \psi_{i-1,j} + \psi_{i,j-1})\\ &+2(\psi_{i+1,j+1} + \psi_{i-1,j+1} + \psi_{i-1,j-1} + \psi_{i+1,j-1})\\ &+6h[(\psi_x)_{i+1,j} - (\psi_x)_{i-1,j} + (\psi_y)_{i,j+1} - (\psi_y)_{i,j-1}]\}\\ &= f_{i,j}.\end{aligned} \tag{3.1a}$$

Here, $(\Delta_h^2)^c\psi_{i,j}$ is a compact second-order approximation for $\Delta^2\psi$. We have also to relate ψ_x and ψ_y to ψ. This is done via the following fourth-order compact schemes.

$$h(\psi_x)_{i,j} = \frac{3}{4}(\psi_{i+1,j} - \psi_{i-1,j}) - \frac{h}{4}[(\psi_x)_{i+1,j} + (\psi_x)_{i-1,j}] \tag{3.1b}$$

$$h(\psi_y)_{i,j} = \frac{3}{4}(\psi_{i,j+1} - \psi_{i,j-1}) - \frac{h}{4}[(\psi_y)_{i,j+1} + (\psi_y)_{i,j-1}]. \tag{3.1c}$$

Equations (3.1a-c) form a second order compact scheme for $\Delta^2\psi$, involves values of ψ, ψ_x and ψ_y at (i,j) and at its eight nearest neighbors, Thus, the scheme is compact. The approximation above is applied at any interior point $1 \le i \le N-1, 1 \le j \le M-1$. On the boundary $i = 0, N$ or $j = 0, M$ ψ, ψ_x, ψ_y are determined from the boundary conditions (2.1b).

The convective term $(\nabla^\perp\psi)\cdot\nabla(\Delta\psi)$ is approximated as follows.

$$(\nabla^\perp\psi)_{i,j} = (-(\psi_y)_{i,j}, (\psi_x)_{i,j}). \tag{3.2a}$$

No further approximation is needed, since ψ_x and ψ_y are part of the unknowns in our discretization. Now,

$$\nabla(\Delta\psi)_{i,j} = ((\Delta\psi_x)_{i,j}, (\Delta\psi_y)_{i,j}) == ((\Delta_h\psi_x)_{i,j}, (\Delta_h\psi_y)_{i,j}) + O(h^2, h^2), \tag{3.2b}$$

where $\Delta_h g_{i,j}$ is the standard approximation for the Laplacian. Note that the above discretization is well defined for any interior point $1 \le i \le N-1, 1 \le j \le M-1$.

The Laplacian of ψ, appearing in the LHS of (3.1a-b), is approximated by $\Delta_h\psi$, where $\Delta_h\psi$ is the standard Laplacian approximation.. The resulting scheme has the following form.

Combining (3.1)-(3.2), we obtain the following scheme.

$$\begin{array}{c} \frac{(\Delta_h\psi_{i,j})^{n+1/2}-(\Delta_h\psi i,j)^n}{\Delta t/2} = \\ -(-(\psi_y^n)_{i,j},(\psi_x^n)_{i,j})\cdot((\Delta_h\psi_x^n)_{i,j},(\Delta_h\psi_y^n)_{i,j}) \\ +\frac{\nu}{2}[(\Delta_h^2)^c\psi_{i,j}^{n+1/2}+(\Delta_h^2)^c\psi_{i.j}^n] \end{array} \tag{3.3a}$$

$$\begin{array}{c} \frac{(\Delta_h\psi_{i,j})^{n+1}-(\Delta_h\psi i,j)^n}{\Delta t} = \\ -(-(\psi_y^{n+1/2})_{i,j},(\psi_x^{n+1/2})_{i,j})\cdot((\Delta_h\psi_x^{n+1/2})_{i,j},(\Delta_h\psi_y^{n+1/2})_{i,j}) \\ +\frac{\nu}{2}[(\Delta_h^2)^c\psi_{i,j}^{n+1}+(\Delta_h^2)^c\psi_{i,j}^n], \end{array} \tag{3.3b}$$

where $(\Delta_h^2)^c$ is defined in $(3.1a-c)$.

4 Stability

4.1 Introduction

This section is devoted to the study of stability and convergence of different schemes like (3.3a-3.3b), when applied to the 1d linear model equation in $[0,1]$

$$\psi_{xxt} = a\psi_{xxx} + \nu\psi_{xxxx}, \tag{4.1}$$

where $a \in \mathbb{R}$, $\nu > 0$. Let us introduce the following finite-difference operators

$$\begin{cases} \delta_x^2\psi_i = \frac{\psi_{i+1}-2\psi_i+\psi_{i-1}}{h^2} & (4.2-a) \\ \delta_x^4(\psi) = \frac{1}{h^4}\{12(2\psi_i-\psi_{i+1}-\psi_{i-1})+6h[(\psi_x)_{i+1}-(\psi_x)_{i-1}]\}, & (4.2-b) \\ \psi_{x,i} = \frac{3}{4h}(\psi_{i+1}-\psi_{i-1})-\frac{1}{4}[\psi_{x,i+1}+\psi_{x,i-1}] & (4.2-c) \end{cases}$$

Notice that we adopt, as in [7] the notation ψ_x for the difference operator (4.2-c), which should not be confused with the operator ∂_x since it operates on discrete functions. Notice also that we adopt only for convenience the notation δ_x^4, but we do not have $\delta_x^4 = (\delta_x^2)^2$.

4.2 Stability of the Predictor-Corrector Scheme

We look now more closely at the time scheme used in our Navier-Stokes schemes. In the context of the model equation (4.1), this scheme reads

$$\begin{cases} \frac{\delta_x^2\psi^{n+1/2}-\delta_x^2\psi^n}{\Delta t/2} = a\delta_x^2\psi_x^n + \frac{\nu}{2}(\delta_x^4\psi^n + \delta_x^4\psi^{n+1/2}) \\ \frac{\delta_x^2\psi^{n+1}-\delta_x^2\psi^n}{\Delta t} = a\delta_x^2\psi_x^{n+1/2} + \frac{\nu}{2}(\delta_x^4\psi^{n+1} + \delta_x^4\psi^n) \end{cases} \tag{4.3}$$

(4.3) is a predictor corrector scheme in time, which handles explicitely the convective term, and implicitely the viscous term (Crank-Nicolson). The discrete spatial operator are given in (4.2). We denote

$$\lambda = \frac{a\Delta t}{h} \quad ; \quad \mu = \frac{\nu\Delta t}{h^2}. \tag{4.4}$$

Proposition 4.1 *The difference scheme (4.3) is stable in the Von Neumann sense under the sufficient condition*

$$|\lambda| \leq \min(2\sqrt{\mu}, \frac{\sqrt{8}}{3}) \tag{4.5}$$

Remark 4.2b: Note that for an Euler time stepping scheme, the stability condition is $6\frac{\nu\Delta t}{h^2} + \frac{a^2\Delta t}{2\nu} \leq 1$.

4.3 Convergence of the Spatially Semi-discrete Scheme

In the next theorem, we show the spatial second order accuracy of the time continuous version of scheme (4.3), when applied to the linear equation (4.1) on $[0, 2\pi[$ in the periodic case.
Define $h = 2\pi/N, x_i = ih, 0 \leq i \leq N-1$. We call l_h^2 the space of N periodic sequences. For $u \in l_h^2$, the scalar product is $(u,v)_h = h\sum_{i=0}^{N-1} u_i v_i$ and the norm $|u|_h = (h\sum_{i=0}^{N-1} |u_i|^2)^{1/2}$. For $\tilde{\psi} \in l_h^2$, the spatial discrete operators $\delta^2\tilde{\psi}$, $\delta^4\tilde{\psi}$, $\tilde{\psi}_x$ are defined in (4.2).

Theorem 4.1 *Let $\psi(x,t)$ be a smooth solution of (4.1), such that $\psi(.,t)$ is periodic on $[0,2\pi]$, and $\psi(0,t) = \psi(2\pi,t) = \partial_x\psi(0,t) = \partial_x\psi(2\pi,t) = 0$. If $\tilde{\psi}(x,t)$ is the solution of*

$$\frac{\partial}{\partial t}\delta_x^2\tilde{\psi} = a\delta_x^2(\tilde{\psi}_x) + \nu\delta_x^4(\tilde{\psi}). \tag{4.6}$$

with initial datum $\tilde{\psi}_i(0) = \psi_0(ih)$, $0 \leq i \leq N-1$. Then, the error $e = \tilde{\psi} - \psi$ satisfies

$$|\delta_x^+ e|_h \leq Ch^2,$$

where δ_x^+ is the forwarded difference operator $(\delta_x^+ e)_i = \frac{e_{i+1}-e_i}{h}$.

5 Numerical Results

We present numerical results for a driven cavity with $\nu = 1/400$. Here the domain is $\Omega = [0,1] \times [0,1]$ and the fluid is driven in the $x-$direction on the top section of the boundary ($y = 1$). I Table 1 we show $max\psi$, $(\bar{x}, \bar{y})$, where $(\bar{x}, \bar{y})$ is the point where $max\psi$ occurs, and $min\psi$. Note that the highest value of the streamfunction at the latest time step is 0.1136. Here the maximum occurs at $(\bar{x}, \bar{y}) = (0.5521, 0.6042)$, and the minimal value of the streamfunction is $-6.498(-4)$. In [4] $max\psi = 0.1139$ occurs at $(0.5547, 0.6055)$, and the minimal value of the streamfunction is $-6.424(-4)$. Figure 1a displays streamfunction contours at $t = 60$, using a 97×97 mesh. In Figure 2a we present velocity components $u(0.5, y)$ and $v(x, 0.5)$ (solid lines) at $T = 60$ compared with [4] (marked by '0'), for $\nu = 1/400$. Note that the match between the results is excellent.

time	quantity	65×65	81×81	97×97
10	$\max \psi$	0.1053	0.1057	0.1059
	$(\bar{x}, \bar{y})$	$(0.5781, 0.6250)$	$(0.5750, 0.6250)$	$(0.5833, 0.6354)$
	$\min \psi$	$-4.786(-4)$	$-4.758(-4)$	$-4.749(-4)$
20	$\max \psi$	0.1124	0.1128	0.1130
	$(\bar{x}, \bar{y})$	$(0.5625, 0.6094)$	$(0.5625, 0.6125)$	$(0.5521, 0.6042)$
	$\min \psi$	$-6.333(-4)$	$-6.371(-4)$	$-6.361(-4)$
40	$\max \psi$	0.1131	0.1134	0.1136
	$(\bar{x}, \bar{y})$	$(0.5625, 0.6094)$	$(0.5500, 0.6000)$	$(0.5521, 0.6042)$
	$\min \psi$	$-6.513(-4)$	$-6.5148(-4)$	$-6.498(-4)$
60	$\max \psi$	0.1131	0.01134	0.1136
	$(\bar{x}, \bar{y})$	$(0.5625, 0.6094)$	$(0.5500, 0.6000)$	$(0.5521, 0.6042)$
	$\min \psi$	$-6.514(-4)$	$-6.5155(-4)$	$-6.498(-4)$

Table 1: Streamfunction Formulation: Compact scheme for the driven cavity problem, $Re = 400$. Ghia et. al. results: $\max \psi = 0.1139$ at $(0.5547, 0.6055)$, $\min \psi = -6.424(-4)$.

In Table 2 we display results for $\nu = 1/5000$. At the latest time level on the finest grid the maximal value of ψ is 0.1160, compared to 0.11897 in [4]. The location of the maximal value is $(\bar{x}, \bar{y}) = (0.5104, 0.5417)$, compared to $(0.5117, 0.5352)$ in [4]. The minimum value of the streamfunction is -0.0029, where the value -0.0031 was found in [4]. Figure 1b displays streamfunction contours at $t = 400$. In Figure 2b we present velocity components $u(0.5, y)$ and $v(x, 0.5)$ (solid lines) at $T = 400$ compared with [4], for $\nu = 1/5000$. Note the excellent match in this case too.

time	quantity	81×81	97×97
120	$\max \psi$	0.1060	0.1068
	$(\bar{x}, \bar{y})$	$(0.5125, 0.5375)$	$(0.5104, 0.5417)$
	$\min \psi$	-0.0028	-0.0028
200	$\max \psi$	0.1117	0.1127
	$(\bar{x}, \bar{y})$	$(0.5125, 0.5375)$	$(0.5104, 0.5312)$
	$\min \psi$	-0.0028	-0.0029
280	$\max \psi$	0.1139	0.1150
	$(\bar{x}, \bar{y})$	$(0.5125, 0.5375)$	$(0.5104, 0.5417)$
	$\min \psi$	-0.0028	-0.0029
400	$\max \psi$	0.1149	0.1160
	$(\bar{x}, \bar{y})$	$(0.5125, 0.5375)$	$(0.5104, 0.5417)$
	$\min \psi$	-0.0028	-0.0029

Table 2: Streamfunction Formulation: Compact scheme for the driven cavity problem, $Re = 5000$ Ghia et. al. results: $\max \psi = 0.11897$ at $(0.5117, 0.5352)$, $\min \psi = -0.0031$.

We also investigated the behavor of the flow for $\nu = 1/7500$ and $\nu = 1/10000$. For $\nu = 1/7500$ at $T = 560$ with a 97×97 mesh. Figure 3a displays streamfunction contours and Figure 4a represents velocity components $u(0.5, y)$ and

$v(x, 0.5)$ (solid lines) compared with [4]. The match is excellent. For $\nu = 1/10000$ at $T = 500$ with a 97×97 mesh- the maximal value of ψ is 0.1190, compared to 0.1197 in [4]. The location of the maximal value is $(\bar{x}, \bar{y}) = (0.5104, 0.5312)$, compared to $(0.5117, 0.5333)$ in [4]. Figure 3b displays streamfunction contours and Figure 4b represents velocity components $u(0.5, y)$ and $v(x, 0.5)$ (solid lines) compared with [4]. Note again that the match is excellent. However, a steady state have not been reached, as we can observe from Figure 5b, which represents the max of the streamfunction from T=400 to $T = 500, \nu = 1/10000$. A similar plot- Figure 5a- shows that for $\nu = 1/7500$ the same quantity grows monotonically towards a steady-state, while for $\nu = 1/10000$ we observe that it grows non-monotonically. A similar phenomena was observed for $\nu = 1/8500$, in agreement with [6] and [5].

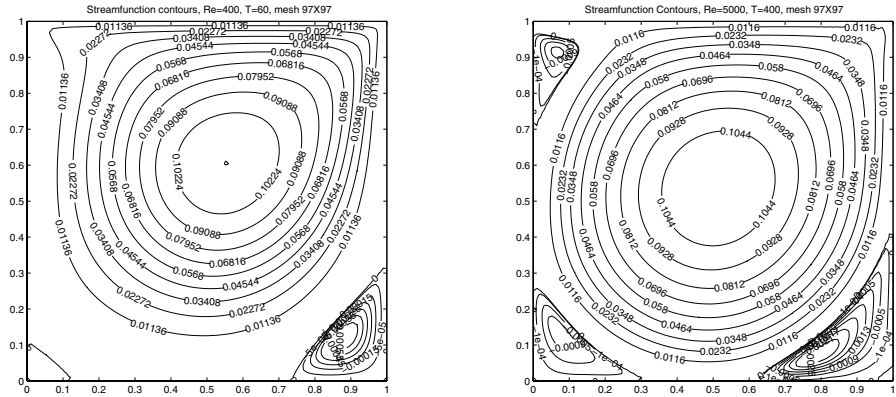

(a) Re=400 (b) Re=5000

Fig. 1. Driven Cavity for $Re = 400, 5000$: Streamfunction Contours

References

[1] I. Altas, J. Dym, M. M. Gupta, and R. P Manohar. Mutigrid solution of automatically generated high-order discretizations for the biharmonic equation. *SIAM J.Sci.Comput.*, 19:1575–1585, 1998.

[2] M. Ben-Artzi, D. Fishelov, and S. Trachtenberg. Vorticity dynamics and numerical resolution of navier-stokes equations. *Math. Model. Numer. Anal.*, 35(2):313–330, 2001.

[3] A. J. Chorin and J. E. Marsden. *A Mathematical Introduction to Fluid Mechanics.* Springer-Verlag, 2-nd edition, 1990.

[4] U. Ghia, K. N. Ghia, and C. T. Shin. High-re solutions for incompressible flow using the navier-stokes equations and a multigrid method. *J. Comp. Phys.*, 48:387–411, 1982.

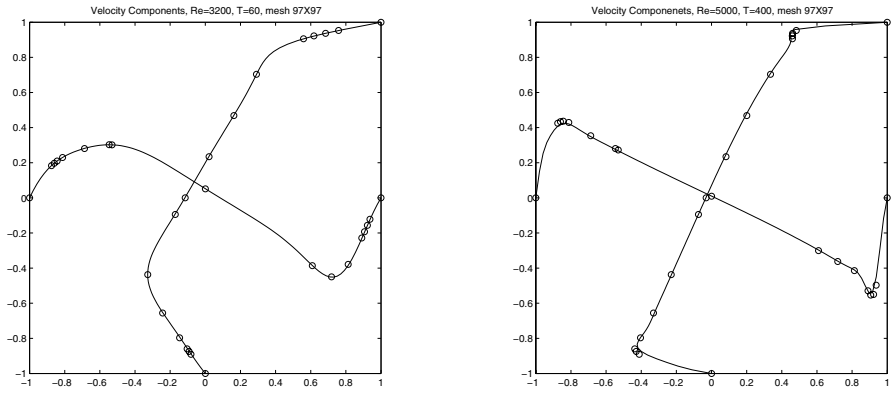

(a) Re=400 (b) Re=5000

Fig. 2. Driven Cavity for $Re = 400, 5000$: Velocity Components. [4]'s results are marked by '0'

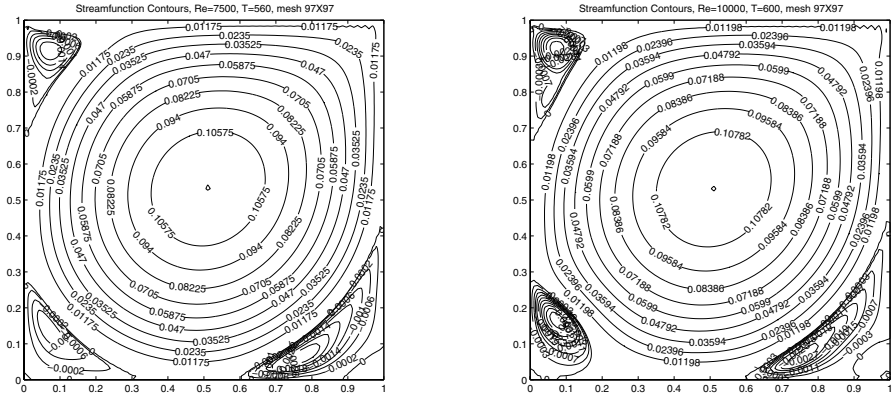

(a) Re=7500 (b) Re=10000

Fig. 3. Driven Cavity for $Re = 7500, 10000$: Streamfunction Contours, $Re = 7500$: max $\psi = 0.1175$, Ghia 0.11998; location is $(0.5104, 0.5312)$, Ghia $(0.5117, 0.5322)$; min$\psi = -0.0030$, Ghia $= -0.0033$. $Re = 10000$: max $\psi = 0.1190$, Ghia 0.1197; location is $(0.5104, 0.5312)$, Ghia $(0.5117, 0.5333)$; min$\psi = -0.0033$, Ghia $= -0.0034$.

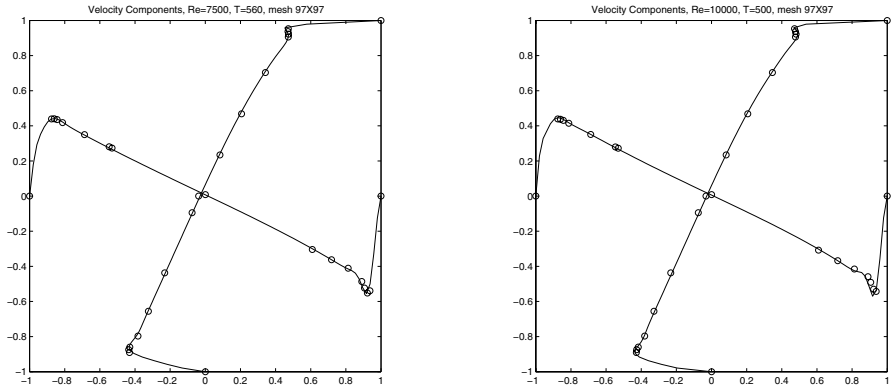

(a) Re=7500 (b) Re=10000

Fig. 4. Driven Cavity for $Re = 7500, 10000$: Velocity Components. [4]'s results are marked by '0'

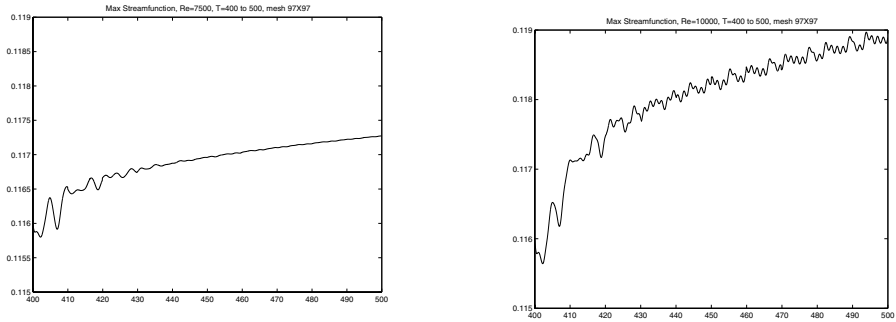

(a) Re=7500 (b) Re=10000

Fig. 5. Driven Cavity for $Re = 7500, 10000$: Max Streamfunction, T=400 to 500.

[5] R. Kupferman. A central-difference scheme for a pure streamfunction formulation of incompressible viscous flow. *SIAM J. Sci.Comput.*, 23, No. 1:1–18, 2001.
[6] T. W. Pan and R. Glowinski. A projection/wave-like equation method for the numerical simulation of incompressible viscous fluid flow modeled by the navier-stokes equations. *Comput. Fluid Dynamics*, 9, 2000.
[7] J. W. Stephenson. Single cell discretizations of order two and four for biharmonic problems. *J.Comp.Phys.*, 55:65–80, 1984.